Multiplicities in ^{16}O-Induced Violent Heavy-Ion Collisions from $5A$ to 2×10^5A MeV

M. I. Adamovich,[13] M. M. Aggarwal,[4] Y. A. Alexandrov,[13] N. P. Andreeva,[1] Z. V. Anson,[1] R. Arora,[4] S. K. Badyal,[8] E. S. Basova,[16] K. B. Bhalla,[7] A. Bhasin,[8] V. S. Bhatia,[4] V. G. Bogdanov,[9] V. I. Bubnov,[1] T. H. Burnett,[15] X. Cai,[18] I. Y. Chasnikov,[1] L. P. Chernova,[17] M. M. Chernyavski,[13] G. Z. Eligbaeva,[1] L. E. Eremenko,[1] A. S. Gaitinov,[1] E. R. Ganssauge,[12] S. Garpman,[11] S. G. Gerassimov,[13] J. Grote,[15] K. G. Gulamov,[17] S. K. Gupta,[7] H. H. Heckman,[3] H. Huang,[18] B. Jakobsson,[11] B. Judek,[14] S. Kachroo,[8] F. G. Kadyrov,[17] G. S. Kalyachina,[1] E. K. Kanygina,[1] L. Karlsson,[11] G. L. Kaul,[8] S. P. Kharlamov,[13] T. Koss,[15] V. Kumar,[7] P. Lal,[7] V. G. Larionova,[13] V. N. Lepetan,[1] L. S. Liu,[18] S. Lokanathan,[7] J. Lord,[15] S. Lukicheva,[17] S. B. Luo,[10] L. K. Mangotra,[8] N. V. Maslennikova,[13] I. S. Mittra,[4] S. Mokerjee,[7] E. Monnand,[6] H. Nasrullaeva,[16] S. H. Nasyrov,[16] V. S. Navotny,[17] G. I. Orlova,[13] I. Otterlund,[11] H. S. Palsania,[7] N. G. Peresadko,[13] N. V. Petrov,[16] V. A. Plyushchev,[9] W. Y. Qian,[18] R. Raniwala,[7] S. Raniwala,[7] N. K. Rao,[8] V. M. Rappoport,[13] J. Ravina,[17] J. T. Rhee,[12] N. Saidkhanov,[17] N. A. Salmanova,[13] F. Schussler,[6] T. I. Shakova,[1] D. Skelding,[15] K. Söderström,[11] Z. I. Solovyeva,[9] K. Staendecke,[12] E. Stenlund,[11] S. C. Strausz,[15] J. F. Sun,[5] L. N. Svechnikova,[17] M. I. Tretyakova,[13] T. P. Trofimova,[16] U. Tuleeva,[16] H. Q. Wang,[18] Z. O. Weng,[5] R. J. Wilkes,[15] G. F. Xu,[2] D. H. Zhang,[10] P. Y. Zheng,[2] S. I. Zhokhova,[17] and D. C. Zhou[18]

(EMU01 Collaboration)

[1]*Institute of High Energy Physics, Alma Ata, U.S.S.R.*
[2]*Academica Sinica, Beijing, People's Republic of China*
[3]*Lawrence Berkeley Laboratory, Berkeley, California 94720*
[4]*Panjab University, Chandigarh, India*
[5]*Hunan Education Institute, Changsa, People's Republic of China*
[6]*Institut des Sciences Nucléaires, Grenoble, France*
[7]*University of Rajasthan, Jaipur, India*
[8]*University of Jammu, Jammu, India*
[9]*V. G. Khlopin Radium Institute, Leningrad, U.S.S.R.*
[10]*Shanxi Normal University, Linfen, People's Republic of China*
[11]*University of Lund, Lund, Sweden*
[12]*Philipps University, Marburg, Germany*
[13]*Lebedev Institute, Moscow, U.S.S.R.*
[14]*Carleton University, Ottawa, Ontario, Canada K1S 5B6*
[15]*University of Washington, Seattle, Washington 98195*
[16]*Institute of Nuclear Physics, Tashkent, U.S.S.R.*
[17]*Physical-Technical Institute, Tashkent, U.S.S.R.*
[18]*Hua-Zhong Normal University, Wuhan, People's Republic of China*

(Received 25 April 1991)

Target-fragment, shower-particle (meson), interacting-proton (36–400 MeV), and total multiplicities in ^{16}O+Ag collisions from $5A$ MeV to 2×10^5A MeV are studied. The target disintegration exhibits energy independence above $100A$ MeV even in the most central collisions. Above $5A$ GeV the energy dependences of the three different categories of particles are similar to those from proton-nucleus interactions. The absolute yield of target fragments is also the same while the yield of protons is twice as large and of shower particles 6–7 times larger in ^{16}O-induced central collisions as compared to p-nucleus reactions.

PACS numbers: 25.70.Np

The collection of data within the EMU01 Collaboration contains an extensive set of analyzed ^{16}O-induced collisions at energies from $5A$ MeV to 2×10^5A MeV. The information about multiplicities of various kinds of particles and fragments is particularly complete. In order to describe the reactions in this wide energy region one must consider phenomena ranging from nuclear structure physics to particle physics in a nuclear environment.

The impact parameter plays an essential role for the dynamical evolution of the collision and thereby for the particle emission [1]. In an asymmetric collision, at impact parameter close to zero, the nuclei will fuse at low energies. At a few tens of MeV per nucleon the fusion process tends to become more and more incomplete and eventually a transition into a fast multifragmentation process appears [2,3]. The disintegration will become more and more efficient with increasing beam energy until the formation time starts to play a role which leads to enhanced transparency for the produced particles. If the stopping of the beam nucleus is large enough, the

TABLE I. Statistics and maximum multiplicities in the various energy bins. The numbers marked with an asterisk are partly based on estimations for $N_T = 2,3$ collisions.

(Energy interval)/A (MeV)	$\langle E \rangle/A$ (MeV)	Number of events with $N_T \geq 4$	Total number of events	Maximum observed N_T	N_s	N_g	N_b
5–15	11.3	84	95*	9	0	0	8
16–35	25.4	155	175*	11	0	0	11
36–75	57.0	541	606*	18	0	3	15
76–128	90.8	421	469*	24	0	9	19
129–179	165	763	847	32	0	10	18
180–220	195	835	926	33	0	12	19
450–470	460	184	203	40	2	18	20
2020–2080	2050	608	664	65	26	31	22
	3700	1568	1686	88	49	45	20
	14600	644	689	125	97	35	20
	60000	486	515	211	176	45	19
	200000	509	534	333	303	31	23

creation of a quark-gluon plasma may occur.

Since the reaction time at high energies becomes small compared to the transverse communication time, a part of the larger nucleus in asymmetric collisions will be left quite undisturbed. For semiperipheral collisions such spectator regions will be discernible except at the lowest energies, where the time is long enough for an effective transfer of mass and energy.

The data presented in this Letter are based on nine different horizontal ^{16}O exposures at six accelerators [GANIL, LBL Bevalac, SATURNE, Dubna Synchrophasotrone, BNL Alternating Gradient Synchrotron (AGS), and CERN Super Proton Synchrotron (SPS)] [4–8] with fluxes of $(5–40)\times 10^3$ ions/cm^2. The collision energies below $0.5A$ GeV are determined from the residual beam range [4] with an error of at most a few percent. Comparisons with p-nucleus data [9–12] at energies above 5 GeV are also presented.

It should be noticed that in all exposures the minimum grain density is large enough to allow for the observation of the particles with the smallest ionization. In the high-energy stacks the forward tracks have been resolved by a second point of inspection and ionization measurement at a large enough distance from the collision. No bias in the total multiplicity of charged particles is therefore expected in any stack.

As a compromise between large enough statistics and small enough collision energy intervals we have divided our data sample into twelve energy bins presented in Table I.

The total number of charged particles (N_T) is further divided into four classes of particles. Normally these classes are strictly defined by energy loss (dE/dx) and range (R) criteria, where dE/dx is measured by grain counting, photometric measurements, or δ-ray counting. In order to include the same kind of particles with respect to their origin both at low and high energies, we use the following classification.

(i) PF particles represent projectilelike (noninteracting) fragments with a charge $Z \geq 2$, classified by the condition $dE/dx \simeq (Z^2/Z^2_{\text{beam}})(dE/dx)_{\text{beam}}$ at the collision point. In addition, it is required that $\beta \simeq \beta_{\text{beam}}$ (from range or constant dE/dx). Z is determined from width or profile photometric measurements or δ-ray counting.

(ii) b (black) particles represent target association (target evaporation particles). They are classified by $R \leq 3$ mm (protons with $E < 26$ MeV) except for short-range PF fragments at low energies which are placed in the previous class.

(iii) s (shower) particles represent produced mesons and noninteracting protons (plus d,t) in the relativistic region. They are classified by $dE/dx < 1.4(dE/dx)_{\text{min}}$.

(iv) g (grey) particles represent interacting singly charged particles corresponding to the proton energy interval 26–400 MeV. They contain all remaining particles, i.e., those with $R > 3$ mm and $dE/dx > 1.4(dE/dx)_{\text{min}}$ ($\beta < 0.7$, participant protons).

Only projectilelike particles with $Z = 1$ will fall into different groups depending on the beam energy. At the lowest energies (mainly the first energy bin) they will fall into the b group, at medium energies ($\sim$ second to sixth energy bins) into the g group, and at the highest energies ($\geq$ seventh bin) into the s group.

The N_T distributions for the twelve energy bins are presented as distribution functions $P(\geq N_T)$ in Fig. 1. Because of the different efficiency for $N_T \leq 3$ events, all distributions are normalized to unity for $N_T = 4$. The steeply falling P functions at low energies get a more and more extended shoulder with increasing collision energy. The largest observed event (see Table I) falls in all cases close to the 10^{-3} level. Typical maximum errors (1 standard deviation) in the interpolated and extrapolated P curves are presented as the shadowed areas in the figure. The original distributions for ^{16}O+emulsion reactions have been renormalized to ^{16}O+Ag collisions [13].

The well-defined $P = 10^{-1}$ and 10^{-2} levels as well as the 10^{-3} level, based on extrapolations, are shown as a function of bombarding energy in Fig. 2. We also show the average N_T value (for ^{16}O+emulsion). The $\langle N_T \rangle$-E relation is (occasionally) well described by one single

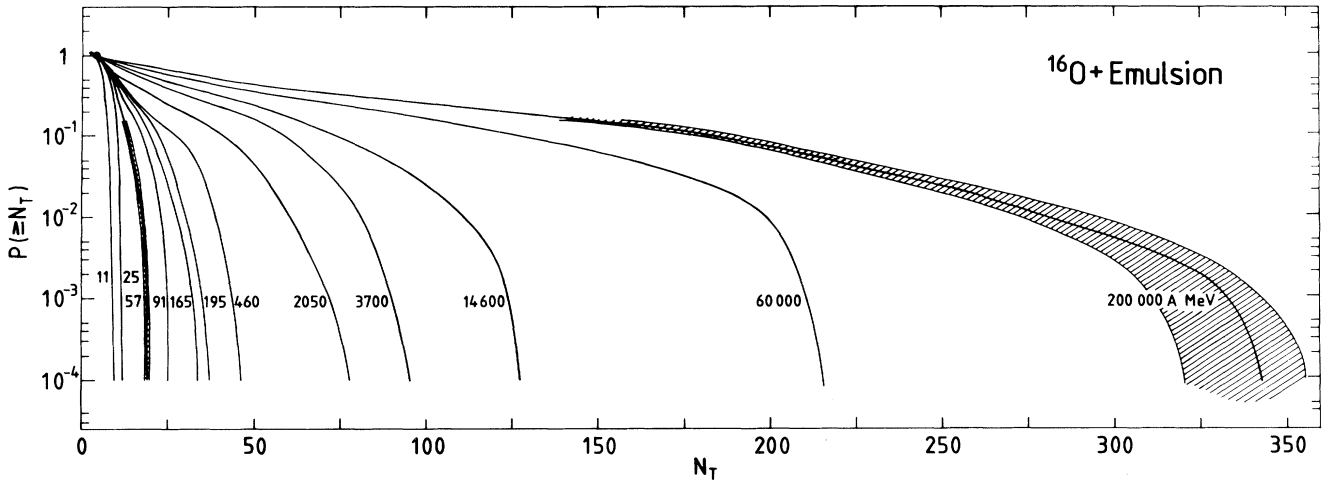

FIG. 1. The distribution functions of N_T for ^{16}O-induced collisions in nuclear emulsion at twelve different energies. The shadowed areas represent statistical uncertainties.

power law in the whole energy interval. In the extreme high multiplicity tail this is only possible for $E \geq 200A$ MeV. A detailed analysis [13] for the low-energy region shows that the transition from fusion to multifragmentation and the onset of pion production cause kinks in the N_T-E relation. The dashed curves and the lowest solid curve ($\langle N_T \rangle$) come from proton-induced collisions [9–12]. These curves, which fall substantially below the corresponding ^{16}O curves, also show a weaker energy dependence due to the different composition of b, g, and s particles.

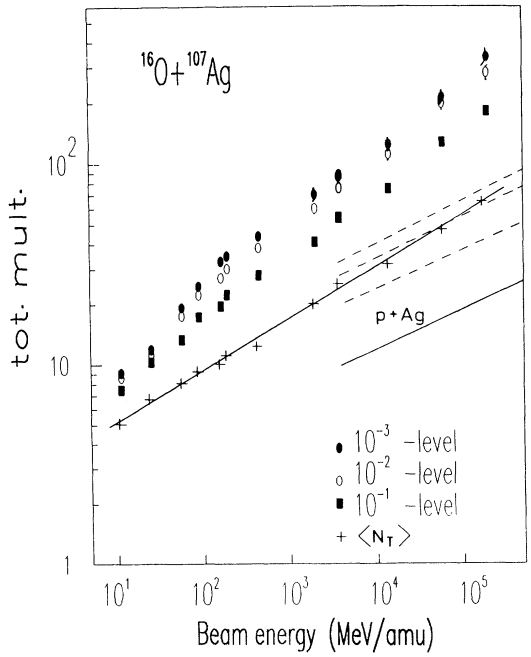

FIG. 2. The 10^{-1}, 10^{-2}, and 10^{-3} levels of the distribution functions of N_T as a function of bombarding energy in ^{16}O+^{107}Ag collisions. +, the average N_T values in ^{16}O+emulsion collisions. The dashed curves as well as the lower solid curve represent the same levels of the distribution functions and $\langle N_T \rangle$ for proton-induced collisions.

The observation of limiting fragmentation in the projectile breakup from $2A$ to $200A$ GeV has been discussed in another paper [14]. All other observations about PF particles in the experiments discussed here are consistent with the results for the b particles, representing the target breakup.

At high energies, the b particles come only from the target disintegration except for a minor contribution from low-energy pions ($E_\pi < 35$ MeV). The maximum possible N_b is thus $\simeq Z_{\text{target}}$ (47 for Ag), but we observe in Fig. 3(a) a maximum N_b value of only $\sim Z_{\text{target}}/2$ even at the $P = 10^{-3}$ level. It is unlikely that peripheral events contribute, due to the strong correlation between large N_b and large N_T. Instead, it is possible that N_b relates only to the nonoverlapping part of the target nucleus ($Z \simeq 30$ for a small impact parameter in a straight-line geometry). A sharp geometrical cut can possibly be believed down to energies of $\sim 1A$ GeV, but we observe in Fig. 3(a) that the saturation of the maximum N_b value is reached already at $\sim 0.1A$ GeV. Below this energy there is a gradual decrease of P for all three levels which is a natural consequence of the fact that the total excitation energy no longer exceeds the binding energy. As mentioned before, fusion is expected at the lowest energies where b particles contain both evaporation particles and preequilibrium particles [13].

The high N_b values for energies between $0.1A$ and $1A$ GeV could be explained in two ways. Either the contribution to N_b from particles coming from the preequilibrium source is gradually getting more important with decreasing energy or the target emission process remains the same also below $1A$ GeV. The observation that proton-induced collisions above 5 GeV give the same constant maximum N_b is intriguing. It could be a pure coincidence that an initial cascade process leaves a remaining target spectator of the same size as in the ^{16}O+Ag case.

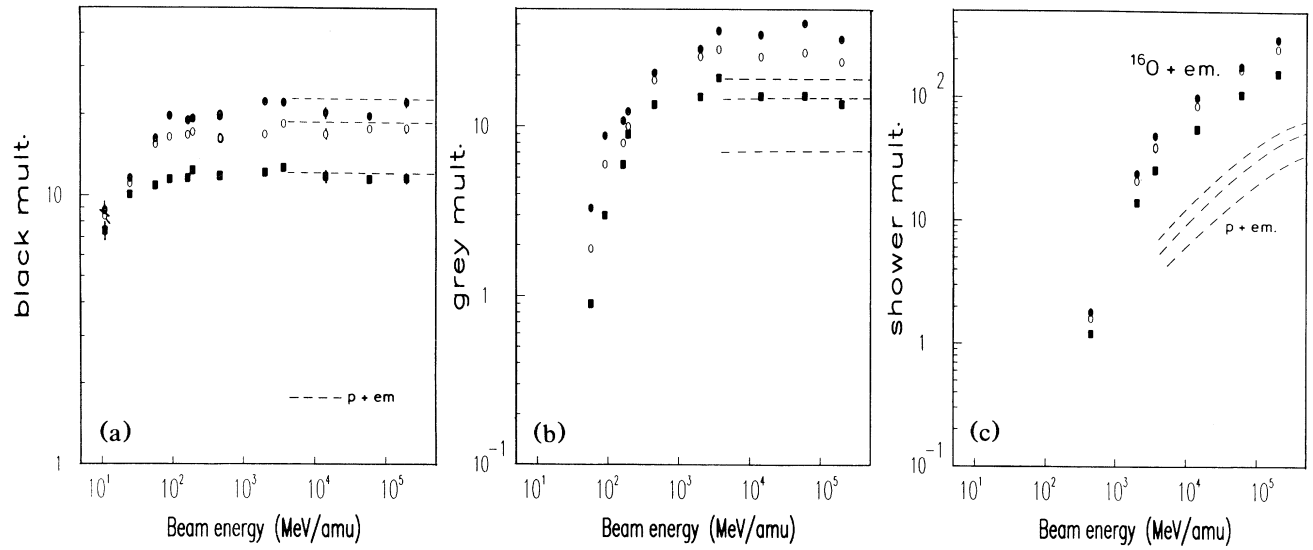

FIG. 3. The 10^{-1}, 10^{-2}, and 10^{-3} levels of the distribution functions for (a) N_b, (b) N_g, and (c) N_s vs bombarding energy for ^{16}O+emulsion collisions. Notations as in Fig. 2.

Detailed comparisons with models which treat the pre-equilibrium processes in a realistic way are necessary to answer these questions.

At incident energies of $\sim 50A$ MeV the production of grey particles starts [Fig. 3(b)]. The N_g distribution exhibits a steeply increasing maximum multiplicity until $\sim 1A$ GeV where a saturation is reached. The g particles are believed to be dominated by protons from nucleon-nucleon (NN) scattering or other fast (preequilibrium) processes. Our data confirm this assumption. The leveling off at high energy is at least partly due to the fact that protons from preequilibrium processes get such high energies that they fall into the s category. Proton-induced collisions above 5 GeV show again a similar energy dependence but the maximum g multiplicity lies a factor of ~ 2 lower. In an independent nucleon-nucleon scattering picture nearly all projectile nucleons interact (e.g., in an optical Glauber calculation). Thus the nucleons meet ~ 8 times fewer "effective" nucleons in the target than the proton. Another explanation is that the number of participant protons scattered into spectator matter comes from the surface of a projectile tube. This gives an $^{16}O/p$ ratio of $\sim 16^{1/3} = 2.5$.

At projectile energies of a few hundred times A MeV the shower particles show up [Fig. 3(c)]. There are two reasons for this; projectile associated protons start to fall in the s region (already at $\sim 100A$ MeV due to the Fermi boost) and the pion production starts. The energy dependence of the shower-particle multiplicity in central ^{16}O+Ag collisions is very similar to that observed in p+Ag collisions. In this case the $^{16}O/p$ yield ratio is $\simeq 7$, i.e., close to $16^{2/3} = 6.3$, which is expected if $N_s \sim$ (participant volume). Comparisons with proper calculations for the early reaction phase are of course necessary both for g and s particles.

In conclusion, we observed that the energy dependence of the average total charged-particle multiplicity follows one single power law in a very wide energy region ($10A$-10^5A MeV) for ^{16}O+ emulsion collisions. The dependence is more complicated for the maximum multiplicity where the fusion-multifragmentation transition and the onset of pion production affect it. The number of black particles increases in the most central collisions up to an energy of $\sim 100A$ MeV and from there it remains constant. The maximum number of grey particles follows the trend which is expected if they originate from interacting nucleons. The shower particles are introduced where the onset of meson production is expected. All multiplicities follow the same energy dependence as observed in proton-nucleus collisions. The maximum multiplicity is the same for target-associated particles while it is a factor of 2 lower for grey particles and a factor of 6-7 lower for shower particles in p-nucleus collisions.

We thank the accelerator staffs of GANIL, SATURNE, LBL Bevalac, Dubna Synchrophasotrone, BNL AGS, and CERN SPS for providing us with high-quality beams. The support from the Swedish Natural Science Research Council, the German Federal Minister of Research and Technology, the University Grants Commission of the Governement of India, the National Science Foundation of China, the Distinguished Teacher Foundation of the State Education Commission of China, the Fok Ying Tung Education Foundation, and the U.S. Department of Energy and the National Science Foundation is gratefully acknowledged.

[1] J. P. Bondorf, in *Proceedings of the Second International Conference on Nucleus-Nucleus Collisions, Visby, Sweden, 1985,* edited by H. A. Gustafsson *et al.* [Nucl.

Phys. **A447** (1986)], pp. 671c–673c.
[2] B. Jakobsson *et al.*, Nucl. Phys. **A509**, 195 (1990).
[3] U. Milkau *et al.*, Gesellschaft für Schwerionenforschung Report No. GSI-91-08, 1991 (to be published).
[4] B. Jakobsson *et al.*, Nouv. GANIL **13**, 8 (1985).
[5] R. Kullberg, K. Kristiansson, B. Lindkvist, and I. Otterlund, Nucl. Phys. **A276**, 523 (1977).
[6] B. Jakobsson and R. Kullberg, Phys. Scr. **13**, 327 (1976).
[7] B. Judek, National Research Council, Ottawa, Report No. HE 3-9, 1978 (unpublished).
[8] M.I. Adamovich *et al.*, Phys. Lett. B **223**, 262 (1989).
[9] H. Winzeler *et al.*, Nucl. Phys. **69**, 661 (1965).
[10] J. Babecki *et al.*, University of Krakow Report No. 929/PH, 1976 (unpublished); (private communication).
[11] I. Otterlund *et al.*, Nucl. Phys. **B142**, 445 (1978).
[12] A. Abduzhamilov *et al.*, Phys. Rev. D **35**, 3537 (1987).
[13] B. Jakobsson *et al.*, Phys. Scr. **38**, 132 (1988).
[14] M. I. Adamovich *et al.*, Phys. Rev. C **40**, 66 (1989).